International Journal of Mechanical, Industrial and Aerospace Sciences
ISSN: 2517-9950
Vol:11, No:1, 2017

Two-Stage Launch Vehicle Trajectory Modeling for Low Earth Orbit Applications

Assem M. F. Sallam, Ah. El-S. Makled

***Abstract*—**This paper presents a study on the trajectory of a two stage launch vehicle. The study includes dynamic responses of motion parameters as well as the variation of angles affecting the orientation of the launch vehicle (LV). LV dynamic characteristics including state vector variation with corresponding altitude and velocity for the different LV stages separation, as well as the angle of attack and flight path angles are also discussed. A flight trajectory study for the drop zone of first stage and the jettisoning of fairing are introduced in the mathematical modeling to study their effect. To increase the accuracy of the LV model, atmospheric model is used taking into consideration geographical location and the values of solar flux related to the date and time of launch, accurate atmospheric model leads to enhancement of the calculation of Mach number, which affects the drag force over the LV. The mathematical model is implemented on MATLAB based software (Simulink). The real available experimental data are compared with results obtained from the theoretical computation model. The comparison shows good agreement, which proves the validity of the developed simulation model; the maximum error noticed was generally less than 10%, which is a result that can lead to future works and enhancement to decrease this level of error.

***Keywords*—**Launch vehicle modeling, launch vehicle trajectory, mathematical modeling, MATLAB-Simulink.

I. Introduction

IMPROVING industry in a developing country facilitates when having a parallel objective related to a space entry mission. Without the LV, no satellite can reach its working orbit and though there would be no space entry missions, which is why it is important to start modeling and design of the LV as the first step on the path of LV production. To achieve an accurate insertion-point for LEO satellites by a small LV, it is necessary to simulate the trajectory track starting from launch through to insertion. Taking into account other perturbation factors that can appear during the atmosphere and space flight, is why it became important to first understand the trajectory design of an LV. At the time of writing this paper, 60 years have passed since the launch of the first satellite (Sputnik 1) [1], and during this long period space technology has changed significantly in many ways, although further improvement is still needed. Launch trajectory parameters remains a topic that has a large amount of research and interest in the space community.

Due to the inherent complexity of an LV, its design is usually separated into different phases, including trajectory, structure, flight control and propulsion. The propulsion system is composed of a large number of components as feed system, working gas, propellants and engines. The structure includes the different stages configuration, fairing size, and separation techniques of faring as well as between the LV stages and the applied forces on the structure considering the material properties. LV flight control contains static and dynamic loops together with location and orientation sensors, and the active actuators to change the LV altitude. The trajectory phase in the LV design is the phase where the present study is focused.

Assem M.F. Sallam is with the Space Technology Center, Cairo, Egypt (e-mail: assemsallam@gmail.com).

Ah. El-S. Makled was with Military Technical College, Cairo, Egypt. He is now with the Space Technology Center, Cairo, Egypt (corresponding author, phone: 2 010 03784889, e-mail: ahmak2007@yahoo.com).

II. Mission Description

It is the analysis of a two stage LV for the trajectory phase design and its validation with a real two stage LV, the real LV case, which is found compatible with the required study, is the Russian LV Zenit-2 [2].

III. Mathematical Modeling

The objective of the powered ascent phase of a space mission is to put the payload, often desired to be as large as possible, into a specified orbit. The manner of how it is carried out is of great importance, as small changes in the overall ascent profile can have significant effects on the final payload that can be delivered, as well as on the design of the ascent vehicle itself, which leads to the deduction of LV motion mathematical modelling. There are two modeling assumptions, which are the diameter of the vehicle geometry is held constant and the dynamic lift of the vehicle is not taken into account. In 2003, K.H. Well introduced a mathematical model for the motion of the European two-stage LV “Ariane 5” [3]. The same model is used in this study, together with ascent flight mechanics proposed by Griffin and French in 2004 [4]. It is modified with the provided flight path profile (trajectory) and mechanical configuration of the Russian LV Zenit-2, a modified model is used to produce the parameters affecting final payload mass versus altitude. An accurate atmospheric model is used to provide variation of ambient temperature and density variation during the LV ascent, which is the Naval Research Laboratory Mass Spectrometer and the Incoherent Scatter Radar Exosphere (NRLMSISE-00) [5]. Selected atmospheric model provides temperature and density variation up to the altitude of 1,000 km with the consideration of launch pad location, time of the year and the current solar activity by the time of launch.

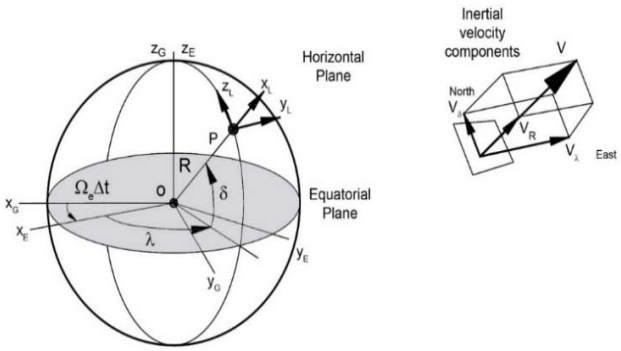

Fig. 1 Definition of Earth and local coordinate systems with parameters relating both coordinates [3]

The used coordinate system is the inertial geocentric axis system with subscript G, as shown in Fig. 1, and the subscript E is for the rotating Earth-fixed axis, their z axes coincides with the Earth's axis of rotation, while subscript L is for the local horizontal axis system, which is attached to the launcher center of mass.

Further analysis is carried on the local axis of the launcher, as shown in Fig. 2, the angle (γ) is the velocity angle, which is the angle between the velocity vector and the northern eastern plane with its center at the launcher center of mass, (θ) is the angle between thrust vector and the north-East plane, the difference between the angle (γ) and (θ) is the angle of attack of the launcher and is denoted by (α). The angle between the projection of the velocity vector and North direction is the (A_z) angle. The drag vector is in the opposite direction of the velocity vector and is denoted by (D).

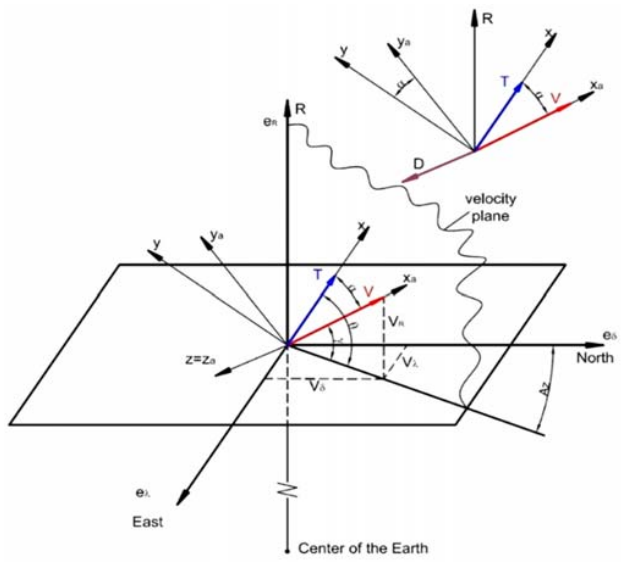

Fig. 2 Thrust, velocity and drag angles on the local inertial coordinates of launcher

Launcher equations of motion, [3] and [4], are deduced based on:

$$\frac{d}{dt}\begin{bmatrix} R \\ \lambda \\ \delta \end{bmatrix} = \begin{bmatrix} V_R \\ \frac{V_\lambda}{R\cos\delta} - \omega_e \\ \frac{V_\delta}{R} \end{bmatrix} \quad (1)$$

$$\frac{d}{dt}\begin{bmatrix} V_R \\ V_\lambda \\ V_\delta \end{bmatrix} = \frac{1}{R}\begin{bmatrix} V_\lambda^2 + V_\delta^2 \\ V_\lambda(V_\delta \tan\delta - V_R) \\ -V_\lambda^2 \tan\delta - V_R V_\delta \end{bmatrix}_L + \frac{\bar{F}}{m} \quad (2)$$

where; R, λ,δ: Inertial position components, m; V_R,V_λ,V_δ: Inertial velocity components, m/s; ω_e: Earth's angular velocity, rad/s; $\bar{F}$: Vectorial sum of all external forces, N; L: Subscript indicating variables in the local coordinate system.

The main forces acting on the LV is gravity and the thrust force generated by engines. There are a variety of types of rocket engines, typically categorized as either high- or low-thrust engines based on the magnitude of the thrust acceleration compared to the local gravitational acceleration. High-thrust engines can provide thrust acceleration magnitudes significantly higher than the local gravitational acceleration. With either type of engine, the rocket mass is not constant, but decreases due to the fact that some mass is expelled out of the rocket nozzle to provide thrust, which is the reaction force in the opposite direction.

There are three types of forces acting on the LV and are applied in the mathematical model, which are the thrust (4), aerodynamic (5), force, (as a function of atmospheric drag) and gravity (6) forces. Principally, the design process must take into consideration that when changing the geometry of the vehicle, not only the mass data changes, but in particular, the aerodynamic data do. Therefore, once a particular change in geometry has occurred, appropriate aerodynamic methods have to be used to recalculate the aerodynamic coefficients in the used model, and the aerodynamic drag used is generated using the USAF automated missile DATCOM (rev 3/99).

The two components in (5) containing the partial derivatives of the side forces and normal forces of the vehicle with respect to angle of attack (α) and sideslip angle (β) are assumed to be negligible if compared to atmospheric drag force, as the lift component and side (wind) slip forces on an LV with its cylindrical shape is very small.

The third acting force is the gravitational force acting on the $\vec{R}$ and $\vec{\delta}$ directions, the component in the $\vec{\lambda}$ direction is almost negligible, which is why it is assumed to be zero.

$$\vec{F} = X\vec{T} + X\,Z\,\vec{F}_{aero} + \vec{G} \quad (3)$$

$$\vec{T} = \begin{bmatrix} g_o I_{spvac}\dot{m}_b(t) - A_e\rho \\ 0 \\ 0 \end{bmatrix}_B \quad (4)$$

$$\vec{F}_{aero} = q\,A_{ref}\begin{bmatrix} -C_D(M) \\ \left(\frac{\partial C_L}{\partial \alpha}(M)\right)\alpha \\ -\left(\frac{\partial C_N}{\partial \alpha}(M)\right)\alpha \end{bmatrix}_B \quad (5)$$

$$\vec{G} = -\frac{\mu}{R^2}\begin{bmatrix} 1+\frac{3J_2}{2}\left(\frac{R_E}{R}\right)^2(1-3\sin^2\delta)+2J_3\left(\frac{R_E}{R}\right)^3(3-5\sin^2\delta)\sin\delta \\ 0 \\ 3J_2\left(\frac{R_E}{R}\right)^2\sin\delta\cos\delta+\frac{3J_3}{2}\left(\frac{R_E}{R}\right)^3(5\sin^2\delta-1)\cos\delta \end{bmatrix}_L \quad (6)$$

The combined force vector (3) is a combined vector of the stated acting forces. The subscript (B) used in (4) and (5) is referred to the body coordinate system that needs to be transferred to the local horizontal axis system (R, λ and δ), that is why, X matrix in (8) is multiplied to the thrust and aerodynamic forces. Transformation matrix Z in (14) is further multiplied to the aerodynamic force to compensate for the angle of attack effect.

$$q = \frac{\rho|\vec{V}_e|^2}{2} \quad (7)$$

$$X = [\bar{e}_x \quad \bar{e}_y \quad \bar{e}_z] \quad (8)$$

$$\bar{e}_x\begin{pmatrix}R\\ \lambda\\ \delta\end{pmatrix} = \begin{bmatrix}\sin\theta\\ \cos\theta\sin Az\\ \cos\theta\cos Az\end{bmatrix} \quad (9)$$

$$\bar{e}_y\begin{pmatrix}R\\ \lambda\\ \delta\end{pmatrix} = \begin{bmatrix}e_z(\lambda)e_x(\delta)-e_z(\delta)e_x(\lambda)\\ e_z(\lambda)e_x(R)-e_z(R)e_x(\delta)\\ e_z(R)e_x(\lambda)-e_z(\lambda)e_x(R)\end{bmatrix} \quad (10)$$

$$\bar{e}_{zo}\begin{pmatrix}R\\ \lambda\\ \delta\end{pmatrix} = \begin{bmatrix}e_x(\lambda)V_e(\delta)-e_x(\delta)V_e(\lambda)\\ e_x(\delta)V_e(R)-e_x(R)V_e(\delta)\\ e_x(R)V_e(\lambda)-e_x(\lambda)V_e(R)\end{bmatrix} \quad (11)$$

$$e_{zm} = \sqrt{e_{zo}^2(R)+e_{zo}^2(\lambda)+e_{zo}^2(\delta)} \quad (12)$$

$$\bar{e}_z\begin{pmatrix}R\\ \lambda\\ \delta\end{pmatrix} = \begin{bmatrix}\frac{e_{zo}(R)}{e_{zm}}\\ \frac{e_{zo}(\lambda)}{e_{zm}}\\ \frac{e_{zo}(\delta)}{e_{zm}}\end{bmatrix} \quad (13)$$

$$Z = \begin{bmatrix}\cos\alpha & \sin\alpha & 0\\ -\sin\alpha & \cos\alpha & 0\\ 0 & 0 & 1\end{bmatrix} \quad (14)$$

Introducing the effect of wind velocity and the Earth's rotation in the direction of the velocity vector (15), results in changing the equivalent velocity vector (V_e) (16), which is out of the velocity plane, as shown in Fig. 3, for simplification the effect of wind velocity is very small if compared to the total velocity, which is why it is neglected from the analysis.

The actual effect of wind is assumed to be zero in the applied model and the effect of the Earth's rotation is only introduced by (17). Equivalent velocity vector (V_e) is projected onto the pitch plane to get the exact velocity component in the direction of launcher movement; the resulting velocity vector is named (V_h) and is expressed by (18).

Transformation matrix K (19) is responsible for the transformation of the out of plane velocity vector (V_e) to the pitch plane. While (A_{zT}) is the azimuth angle of the thrust vector.

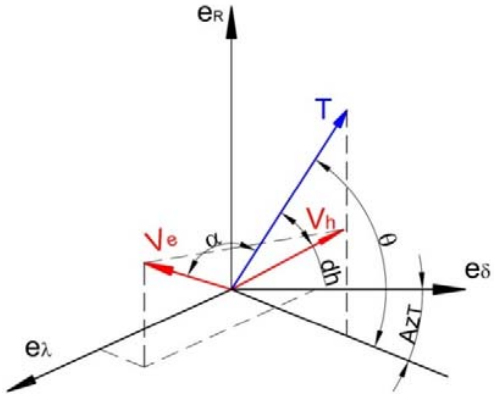

Fig. 3 Equivalent velocity (V_e) vector under effect of wind velocity and its projection (V_h)

$$\vec{V} = \sqrt{V_R^2+V_\lambda^2+V_\delta^2} \quad (15)$$

$$\vec{V}_e = \vec{V} - \vec{V}_a \quad (16)$$

$$\vec{V}_a = \vec{\omega}_e R\cos\delta - \vec{w} \quad (17)$$

$$\vec{V}_h = K\vec{V}_e \quad (18)$$

$$K = \begin{bmatrix}1 & 0 & 0\\ 0 & \sin^2 Az_T & \sin Az_T\cos Az_T\\ 0 & \sin Az_T\cos Az_T & \cos^2 Az_T\end{bmatrix} \quad (19)$$

where; A_{ref}: Surface area of launcher subjected to drag, m^2; C_D: Launcher drag coefficient; C_L: Launcher lift coefficient; C_N: Launcher side slip coefficient; $\bar{F}_{aero}$: Aerodynamic forces, N; $\bar{G}$: Gravitational forces, N; $\bar{T}$: Thrust vector, N; $\bar{w}$: Wind velocity vector, m/s.

A MATLAB code is developed in order to simulate the LV trajectory by resolving numerically the equations of motion. This program enables the performance calculations to be carried out. By changing the LV input or design parameters, a change in the overall performance can be investigated to find the optimum parameters that satisfy the mission requirements.

The forces acting on a LV are the thrust, the aerodynamic forces, the gravitational attractions, as well as the wind and solar radiation pressure. The two last forces are usually small and are therefore neglected. In this study, the rocket trajectory is considered as three dimensional. This assumption has been made because the tool developed to simulate the LV trajectory has to be relatively simple and fast to understand the effect parameters.

To proceed with the LV mathematical model, some angles are introduced to the model. These angles represent variation of the LV orientation during its flight path. As shown in Fig. 4, there are number of angles that need to be introduced in the model. Starting with the LV angle of attack (α), which is the angle between the LV velocity vector (angle γ) and the thrust vector (angle θ), angle variation differs from one stage to the other, so that during the LV first stage, it is controlled mainly by the LV velocity, which is represented by the Mach number,

then the main influencing factor is the maximum allowable angle of attack the LV can withstand.

There are two values of (α), the first one is the real angle of attack (20), where the LV encounters atmospheric conditions, this angle contributes in the calculation of the aerodynamic force that drags the LV under the effect of atmosphere. The second form of this angle is its projection onto the pitch plane, it is denoted (α_h) (21), having the same subscript of velocity vector when also projected to the pitch plane. This angle is used in the calculation of the LV flight path angle (θ).

$$\alpha = \cos^{-1}(\sin\theta \sin\gamma_e + \cos\theta \cos\gamma_e \cos(Az_e - Az_t)) \tag{20}$$

$$\alpha_h = \begin{cases} 0 & M_h < 0.05 \\ -\frac{\alpha_{max}}{0.0082}(M_h - 0.05)^3(M_h - 0.8)^2 & 0.05 \le M_h \le 0.8 \\ 0 & M_h > 0.8 \end{cases} \tag{21}$$

$$M_h = \frac{|\bar{V}_h|}{a} \tag{22}$$

$$a = \sqrt{\gamma \frac{R}{M} T} \tag{23}$$

where; a: Speed of sound, m/s; Az_e: Velocity vector azimuth, rad.; Az_t: Thrust vector azimuth, rad.; R: Gas constant, J/kg.K; M: Molecular weight of air; T: Temperature, K; γ: Specific heat ratio.

Molecular mass of air used in (22) is changed by the increase of altitude. Table I shows the variation of the molecular mass for different altitudes.

The azimuth of the velocity and thrust vectors are measured counter clock-wise from the north direction, and the angle between two azimuth vectors is used in the calculation of the angle of attack (20), these angles are calculated by using (25) and (26).

TABLE I
M VARIATION

H, km	M
0	0.02897
12	0.02897
14	0.02897
24	0.02897
28	0.02897
80	0.02897
90	0.02897
100	0.0289
120	0.02871
140	0.02845
160	0.02804
180	0.02736
200	0.02632
300	0.02195
400	0.01956
500	0.01828
600	0.01752
700	0.01703

$$Az_o = \sin^{-1}\left(\frac{\cos i}{\cos\delta_i}\right) \tag{24}$$

$$Az_t = \begin{cases} Az_i, & t = 0 \\ \sin^{-1}\left(\frac{\cos\delta_i \sin Az_i}{\cos\delta}\right), & t > 0 \end{cases} \tag{25}$$

$$Az_e = \tan^{-1}\left(\frac{V_{\lambda e}}{V_{\delta e}}\right) \tag{26}$$

Velocity angle (γ) change during the LV flight is a major angle for indicating the final orbit of the LV payload after separation. Flight path angle (θ) is related to the velocity angle (γ) during the first stage flight, but it is significantly changed deliberately by the LV control for the adjustment of separation conditions.

Separation conditions are clearly identified by having a radial component of velocity equal to zero, which is guaranteed by having the angle (γ) at the burnout point approximately near zero, the orbit required for the payload has a predefined velocity and inclination, and separation velocity should be as close as possible to the required orbital velocity to assure minimum orbital transfer velocity budget spent by the satellite propulsion system, which increases the satellite lifetime as well as facilitating the transfer to the designed working orbit.

As shown in Fig. 4, angle (γ) and (θ) starts with a vertical angle from the surface of the Earth (90°) (tet_gam_i), then there will be a little shift between the angles (γ and θ) just after LV lift-off this small difference between the angles are under the effect of Earth's rotational velocity, as shown in (17).

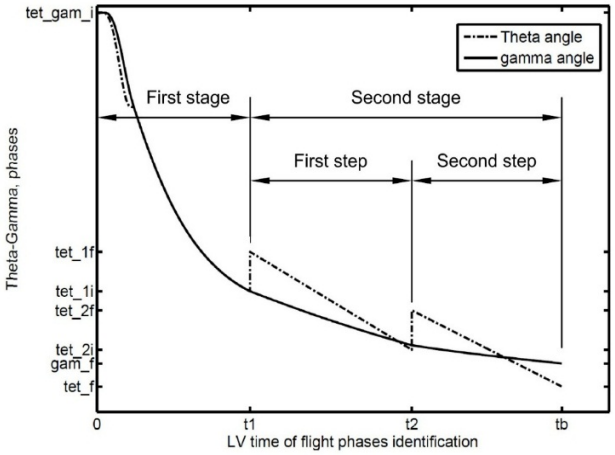

Fig. 4 Change of flight path and pitch angles (θ) and (γ) over the whole flight of the LV

At the burnout of the first stage at time (t_1), the LV flight path angle is re-positioned by a gimballed engine (control engine) to a designed angle (tet_1f), change of flight path angle through the first step phase is quadratic or linear for approximation, rate of change of (θ) angle through this phase is also a designed control parameter that the LV control system should monitor and execute. In most of the LVs, the second stage flight path variation is a one-step variation, but the mathematical model described is tailored on the Zenit-2 LV, which has the division of the second stage flight path angle into two equal sections (27), where the time of the first step is equal to time of second step, so that by the end of the first step and at time (t_2), another

angled force is performed by the control engine to change the flight path angle to a predefined designed value (tet_2f) and the flight path angle continues also with another rate of change, which is another designed control parameter that ends by the burn-out point of the second stage engine at time (t_b). The initial azimuth (Az), the maximum angle of attack (α_{max}), the initial pitch angle before the second stage ignition (tet_1i and tet_2i) and the pitch angle rate at the second stage ignition, should be chosen to achieve the required inclination of separation (parking) orbit, the specified final conditions at the burnout point should satisfy the condition that ($\gamma_b \approx 0$) with the maximum payload mass at the specified burn-out altitude.

$$\theta_2 = \theta_{1i} + \Delta\theta_{1i} + \dot{\theta}_1(t_2 - t_1) + \Delta\theta_{2i} + \dot{\theta}_2(t_b - t_2) \quad (27)$$

$$\gamma_h = \tan^{-1}\left(\frac{V_{hR}}{\sqrt{V_{h\delta}^2 + V_{h\lambda}^2}}\right) \quad (28)$$

$$\theta_{1i} = \gamma_h + \alpha_h \quad (29)$$

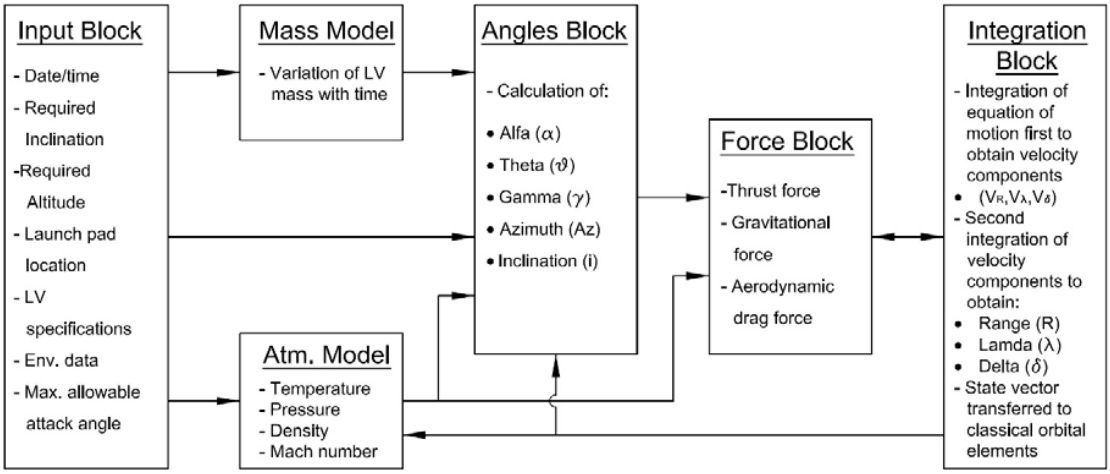

Fig. 5 The mathematical model block diagram

IV. Mathematical Model Implementation and Results

The deduced mathematical model is implemented on Simulink, which is a MATLAB based application. The built model is simplified in the block diagram shown in Fig. 5, it consists of six main blocks (input, mass, atmospheric, angles, force and integration), where the input parameters are taken from a Russian LV Zenit-2 [2], and used to feed all the system blocks. In the angle block, all the LV orientation angles are calculated and used as an input to the force block, which together with the atmospheric data outputs the forces acting on the LV body during flight. Force vectors are fed to the integration block where the velocity and position vectors (LV state vector) are calculated and loop back data are returned to the system blocks to sense the change in the LV state vector.

Expressing the velocity variation over the whole flight time is carried out using the absolute and Earth relative velocity magnitudes, as shown in Fig. 6. Absolute velocity starts with the Earth's rotational velocity (Earth kick) with a value 426 m/s, velocity then increases gradually until it reaches 3257 m/s by the end of first stage. As the loading factor at the beginning of second stage is quite low (approximately one) and the second engine characteristic is of lower thrust than the first stage engine, the velocity rate of change during the second stage is smaller than that of the first stage, which is clear with a smaller slope, the velocity keeps on increasing during the second stage until it reaches the separation velocity 7784.26 m/s.

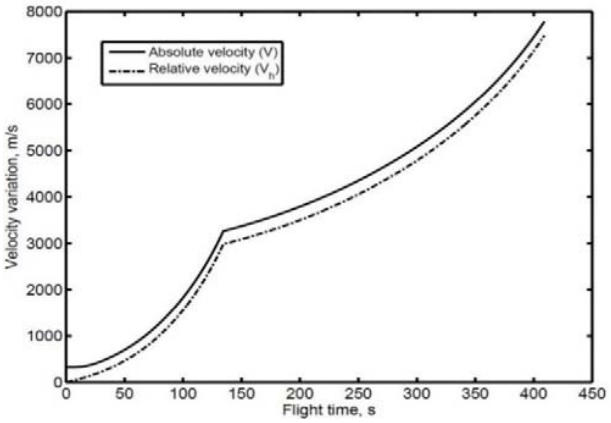

Fig. 6 Velocity profile of Zenit-2 showing absolute and relative velocities

The reached velocity at separations differs from the corresponding altitude (181 km) circular orbit velocity (7795.5 m/s) by 11.3 m/s with an error about 0.15 % from the required velocity, the difference in the reached velocity results in placing the spacecraft in an elliptical orbit, and should be corrected by the spacecraft's propulsion system. Relative velocity curve is nearly the same as the absolute velocity curve but showing the starting velocity to be zero, which is relative to the Earth's rotational velocity, the difference remains approximately the same during the whole flight time of the LV.

There is a velocity component which is important to be

discussed, Fig. 7, this component is the radial component. By reaching the required altitude of spacecraft separation (parking orbit), spacecraft should be separated with zero radial velocity to avoid gaining the spacecraft any extra altitude than designed, while the tangential velocity having the required circular velocity of the reached orbit. Fig. 7 shows the maximum value by the time of separation of the first stage, followed by the dropping in its value during the second stage; the effect of change on the flight path angle is clear in the changing slope of the curve, the final radial velocity is -3 m/s, which is a small value that is fully eliminated by the satellite thrusters after the separation during the damping process. Radial velocity error can increase until reaching the total available velocity of the corresponding altitude (7794.5 m/s); that is why the error is 0.03%, referring to the corresponding altitude circular velocity.

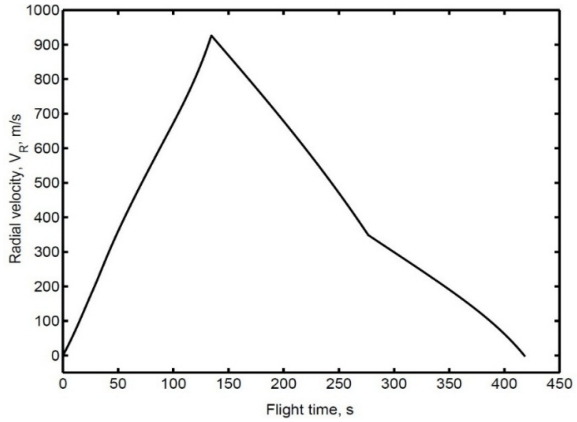

Fig. 7 Radial velocity variation over Zenit-2 flight time

The main target of using the LV is to deliver its payload (spacecraft) from the ground (Earth's surface) to a certain altitude, so, the reached altitude with the required velocity is nearly the main goal of LV, altitude variation during the LV flight time is expressed by three curves, as shown in Figs. 8-10. Fig. 8 shows the variation of altitude with the corresponding ground range, Figs. 9 and 10 express the altitude and ground range over the LV flight time, respectively.

As shown in Fig. 8, there is the altitude variation of different stages of LV with the corresponding ground range. Fairing separation starts at time 83 s at an altitude 24 km, at this moment the fairing trajectory will take the shape of a projectile, where the altitude will continue to increase until it reaches a maximum value of 77.62 km at the time of 142.7 s, finally the fairing returns back and hits the ground at the time of 236.3 s with a 163.3 km ground range far from the launch pad. First stage separation starts after 134.5 s from the LV lift-off at an altitude 62.2 km after passing a ground range of 113 km; after separation, the first stage structure also continues its trajectory as a normal trajectory until it reaches an altitude approximately outside the atmospheric layer (115.8 km) at a ground range 434 km after a time of 250.2 s, it returned back to earth with a total ground range 875.3 km after 413.2 s.

Second stage trajectory differs from that of the fairing and LV first stage, it is designed to deliver the payload (satellite) to the required altitude with the orbit velocity; the whole flight path trajectory is actively powered by the engines of the first and second stages. Total flight time of the second stage is 410.3 s and the final altitude reached is 181 km with a corresponding ground range of 1348.5 km.

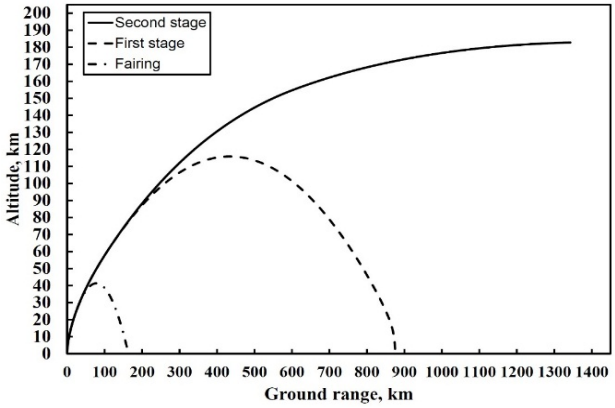

Fig. 8 Altitude variation with ground range for the first, second stages and fairing of LV from Baikonur

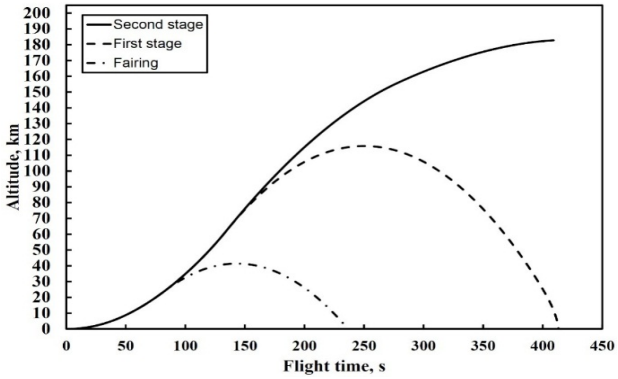

Fig. 9 Altitude variation with flight time for the first, second stages and fairing of LV from Baikonur

In Figs. 9 and 10, the added perspective to the altitude-ground range is the time of the flight during each stage. The time of flight of the first stage is slightly more than the second stage, while the ground range is greatly smaller than that of the second stage. The collection of data for the different stages relating to the altitude and ground ranges as well as the flight time, are shown in Table II.

TABLE II
FLIGHT SEGMENTS OF DIFFERENT LV STAGES

	Flight segment	Time, s	Ground range, km	Altitude, km
Fairing	Separation	83	23	24.2
	Maximum altitude	142.7	77.6	41.4
	Final destination	236.3	163.3	0
First stage	Separation	134.5	113	62.2
	Maximum altitude	250.2	434.1	115.8
	Final destination	413.2	875.3	0
Second stage	Final destination	410.3	1348.5	181

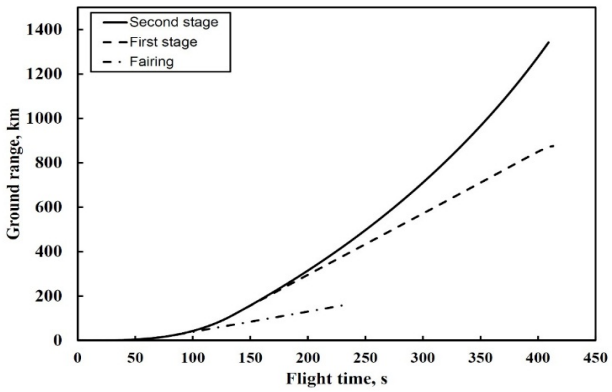

Fig. 10 Ground range variation with flight time for the first, second stages and fairing of LV from Baikonur

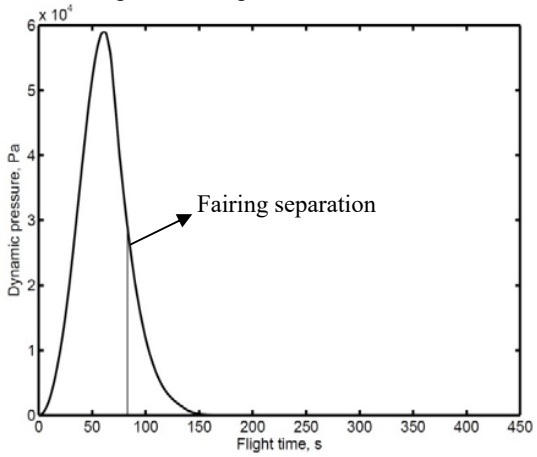

Fig. 11 Dynamic pressure variation showing location of fairing separation

TABLE III
ZENIT-2 MASS DISTRIBUTION

Description	mass, kg	Description	mass, kg
First stage structure	32660	Second stage propellant	82270.54
First stage propellant	322000	Fairing	250
Second stage structure	9329.46	Payload	14000
Total		460510	

During the flight of the LV and in the same time sequence, there is the payload fairing and the first stage of LV that are separated according to the designed conditions.

Payload fairing withstands and protects the payload from harsh surrounding loads that cause excess overheating of the payload (satellite) under the effect of friction at high velocities and the maximum aerodynamic loading, which takes place at the maximum dynamic pressure. Separation of the payload fairing is based on passing the maximum dynamic pressure, and at the mid time of the dynamic pressure drop separation takes place. Fig. 11 shows the dynamic pressure variation during the LV flight time, with maximum dynamic pressure 5.9 x 10^4 Pa after 61 s; then dynamic pressure drops down to reach its minimum near zero value after 150 s [6], [7]. Separation of the LV first stage takes place when the amount of propellant available ceases to operate the first stage engine.

The LV starts its ascent or lift-off with the flight path "thrust" (θ) and pitch "velocity" angles (γ) at 90º, which shows the vertical ascent. There is a little shift between LV longitudinal axis and the flight path (shift between θ and γ) under the effect of Earth's angular velocity that produces a component out of flight plane and the LV coincides with the flight path again after 33 s from lift-off. The LV continues without any drift until the end of first stage, which ends with a flight path angle (tet_1i) equal to 18º, as shown in Fig. 4; the related value stated in the Zenit-2 LV [2] for the first stage final flight path angle is 20º with an error 10%.

The second stage flight path angle (θ) is designed to have two step changes; the first step is at the beginning of the stage and the second at the middle of the stage. It is chosen to increase the angle (θ) by 10º initially at both steps, this step value is selected with the linear rate of change ($\dot{\theta}$) to guarantee that by the end of each step that the value of angle (θ) coincides with the pitch angle (γ), a matter that assures the maximum angle of the attack not to be increased than 10º. By the end of the flight time, the angle (θ) reaches a value -5.5º, a value that helps the radial component of velocity to be very close to zero (-3 m/s).

The pitch angle (γ) describes the main trajectory of the LV, and is the angle where the angle (θ) is connected during the design of LV trajectory; it also started with vertical ascent (90º) and continues to decrease during the flight path until it reaches a value of 0.1º by the end of the flight path.

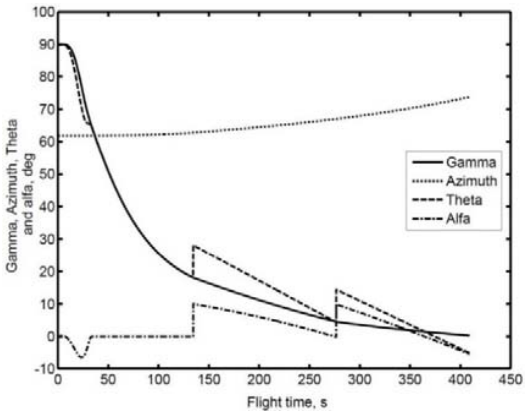

Fig. 12 Gamma, Azimuth, theta and Alfa angles variation over flight time

Angle of attack (α), Fig. 12, is stated to have a maximum allowable value of 10º [2]. It starts with a zero angle and decreases during the initial phase of the flight to -6.5º, then it returns back to the zero angle of attack until the start of the second stage; a pattern that is confirmed confirms with Saqlain Akhtar [8], where the induced step of angle (θ) is introduced, at this time the angle of attack reaches its maximum value (10º) then it returns gradually during the first step phase to the zero value, at the beginning of the second step phase, the angle of attack started with 10º and decreases gradually with a rate of change of more than that in the first step to end with a value -6.5º.

The azimuth of the launch changes according to the launch pad latitude and the required inclination of the final insertion point of the satellite. Thus, for the launch pad placed at Baikonur at a latitude of 45.943° and the required inclination 51.6°, as shown in Fig. 12, the azimuth starts with a value 61.9° and increases slightly during the whole flight time with approximately 12° to reach a value of 73.8° by the end of flight.

LV initial lift-off mass is 460510 kg [2]. The structure and propellant masses of the two stages together with the masses of payload and fairing are shown in Table III. The first stage propellant is consumed with a mass flow rate 2394.7 kg/s, thus, the first stage propellant is totally consumed after 134.5 s, as shown in Fig. 13, which is the time where the first stage is separated from the LV and the second stage engine starts to operate and continues consumption of the propellant with a rate very small compared to the burning rate of the first stage engine 259.39 kg/s; it continues burning for 275.5 s where the total flight time of the LV is ≈ 410 s. The fairing separation is after 83 s from lift-off; this separation cannot be indicated from Fig. 13 as the mass of fairing (250 kg) is too small compared to the mass of LV (approx. 460 tons).

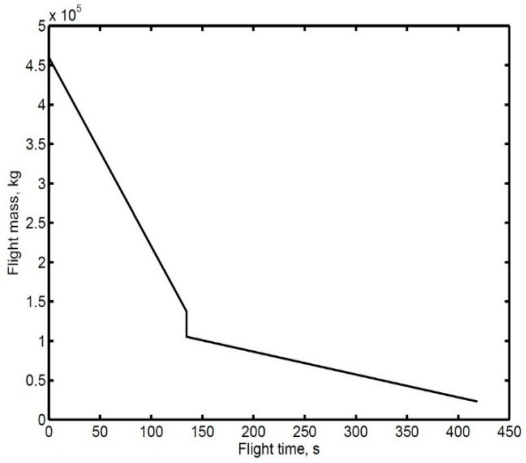

Fig. 13 LV in flight mass drop during flight

V. Conclusion

A verified tool is presented in this paper, which is used to assist the trajectory design parameters of an LV capable of inserting a small satellite into space. The tool is implemented using MATLAB-Simulink software, which includes a mass variation model, an atmospheric model with ambient parameters variation up to the altitude of separation, dynamic motion model including the state vector variation and the different flight angles for the whole flight time of the LV.

The trajectory is divided into three distinct phases, the vertical ascent, as well as the gravity turn and lastly the controlled flight program. A simplified drag model is used, where the drag coefficient only varies with the Mach number.

The modelled LV reached a final separation altitude with separation conditions to an altitude with an error 9.5% from the Zenit-2 LV (200 km altitude); the difference in the altitude yields a difference in the final velocity value by an error of about 0.15%. Separation conditions for a satellite are guaranteed within a limit, with a radial velocity -3m/s and a flight path angle -5.5m/s.

The model validation is important to determine the accuracy of the results obtained. In this study, the model validation is shown with an overall error less than 10% in regards to the Zenit-2 LV data [2]. An error that can be improved in future studies related to LV trajectory.

References

[1] Roger R., Donald D., Jerry E., "Fundamentals of Astrodynamics", Dover publications, New York, 1971.
[2] Kirsanov V. G., "Tutorial on Ballistics to do the academic year work for post graduate students ", Moscow aviation institute, 1981.
[3] K. H. WELL, "Neighboring Vehicle Design for a Two-Stage Launch Vehicle" University of Stuttgart, 70550 Stuttgart, Germany,2003.
[4] Michael D. Griffin, James R. French, "Space Vehicle Design", second edition, AIAA Education Series, Reston, Virginia, 2004.
[5] J. M. Picone, A. E. Hedin 1, and D. P. Drob, "NRLMSISE-00 Empirical Model of the Atmosphere: Statistical Comparisons and Scientific Issues", E. O. Hulburt Center for Space Research Naval Research Laboratory Washington, DC 20375, 2001.
[6] Greg A. Dukeman and Ashley D. Hilly, "Rapid Trajectory Optimization for the ARES I Launch Vehicle", AIAA 2008-6288, AIAA Guidance, Navigation and Control Conference and Exhibit 18 - 21 August 2008, Honolulu, Hawaii, 2008.
[7] XUAN Ying†, ZHANG WeiHua and ZHANG YuLin, "Pseudospectral method based trajectory optimization and fairing rejection time analysis of solid launch vehicle", Sci China Ser E-Tech Sci, vol. 52 | no. 11 | 3198-3206, 2009.
[8] Saqlain Akhtar and He Linshu, "Support Vector Machine Based Trajectory Metamodel for Conceptual Design of Multi-Stage Space Launch Vehicle", School of Astronautics Beihang University, 37-XueYuan Lu 100083, Beijing, China, 2005.

Assem M.F. Sallam received a B.S. in Engineering from Military Technical College, Cairo in 2000. Completed Master degree in 2008, currently a PhD student since 2015. Worked in the field of aeronautics since graduation and currently working in the field of space specialized in orbital mechanics.

Ahmed El-S. Makled is a PhD academic doctor, worked in the aerospace engineering field, specialized in rocket propulsion, launch vehicle design and satellite launch services.